Consiglio Nazionale delle Ricerche
National Research Council of Italy

Istituto di Geoscienze e Georisorse
Institute of Geosciences and Earth Resources

SegemAR
Servicio Geológico Minero Argentino

SOCOMPA GEOTHERMAL PROSPECT
Report on waters geochemistry

Elaborated by:
Dr. Matteo Lelli

Institute of Geosciences and Earth Resource (IGG)
National Research Council (CNR-Italy)

August 2018

1. Introduction

This report regard the elaboration and interpretation of the results of chemical and isotopic analyses carried out on water samples collected from cold and thermal springs in the Socompa Geothermal Prospect (SGP), Salta Province (Argentina). Sample collection was carried out in a field campaign that took place between April 20th-25th , 2018.

In the SGP just a single geochemical exploration study was performed (Galliski et al., 1987), but geochemical data for thermal waters collected seems to be disappeared or unavailable. Therefore, in order to get more information regarding the origin and evolution of thermal waters circulating in this area:

- particular attention was addressed to the identification and sampling of cold and fresh waters from springs considered suitable to study the probable source areas (also sampled very far from the SGP, as for samples SO14, SO15 and SO16). These samples were included only in the elaboration of stable isotopic data, since their chemistry is governed by physico-chemical processes active in different geological context (far from SGP) and it is not representative of the local conditions present in the SGP. Conversely, the isotope composition of these waters could be useful for better understanding of the evolution of waters that feed the local thermal circuits;
- the geochemical investigation was enlarged in the Salar of Llullaillaco (located ≈35Km S-SW to the Socompa Volcano), in which some thermal/warm springs were previously identified;
- some previous data regarding samples from rain and surface water collected in the closed basins of the Atacama Desert (Northern Chile – Alpers and Whittemore, 1990) were included in the elaboration (even if just isotopic composition was analyzed).

2. Geochemical field work and laboratory analyses

Prior to and during the field work particular attention was focused on the identification of cold and thermal springs located abroad of the studied area, never sampled before or completely unknown. The perimeter of the Socompa lagoon was totally travelled and great part of the Llullaillaco salar was visited. The study area represents a semi-arid region located at very high altitude and small number of springs are available for sampling.

A geochemical survey of the SGP was carried out in April 2018. A total of 24 water samples were collected: 12 from thermal springs, 1 from thermal well located in the Salar of Llullaillaco, 1 from the Laguna Socompa, 6 from cold springs and 4 from salty springs located around it (see Fig.A1 and A2). Since the weather not assured to climb the Socompa volcano in safety conditions, gas samples from fumaroles located close to the summit were not collected.

For what concerns the samples collected, both an untreated aliquot (one 50 mL bottle and one 125 mL bottle) and a filtered-acidified aliquot (one 50 mL bottle and one 125 mL bottle) were stored in new polyethylene containers. Filtration was performed using 0.45 μm membranes of cellulose acetate and acidification was accomplished by addition of HNO_3 1:1 (1 mL in 50 mL). For thermal springs an aliquot acidified with 1ml of HCl 1:1 in amber glass bottles was also collected for NH_3 analyses.

Temperature, pH, total alkalinity (acidimetric titration), and electrical conductivity were measured in the field by means of portable instruments (see Fig.A3a and A3b). Flow rate was evaluated where possible. The pH-meter was calibrated against two pH buffers with nominal pH values of 4 and 7. The analytical uncertainty for pH is less 0.05 units. Physico-chemical parameters measured in the field are reported in Table 1.

Chemical and isotopic analyses of water samples were carried out in the laboratories of the Institute of Geosciences and Earth Resources of the Italian National Research Council, Pisa (IGG-CNR) as follows:

(i) Li^+, Na^+, K^+, Mg^{2+}, Ca^{2+} and B in the filtered-acidified aliquot by Inductively Coupled Plasma-Optical Emission Spectroscopy, using an ICP-OES Perkin-Elmer Optima 2000 DV;

(ii) Cl^-, Br^-, F^-, SO_4^{2-}, and NO_3^- in the untreated aliquot by ion chromatography (IC) employing an IC Metrohm 883 Plus;

(iv) NH_4^+ in the acidified aliquot by ion-selective electrodes utilizing a pH-mV meter Orion Research Expandable ion Analyzer EA920;

(v) dissolved SiO_2 in the filtered-acidified aliquot by visible spectrophotometry using an UV-VIS Spectrophotometer Jasco V-530;

(vi) the isotope ratios $^{18}O/^{16}O$ and $D/^1H$ of water in the untreated aliquot by Mass Spectrometry, utilizing an MS Europa Scientific - mod. Geo 2020 and a Los Gatos Research DL-100;

Short-term analytical precision (repeatability) is better than 2% for ICP-OES analyses, 3-5% for IC and ISE determinations, and close to 5 % for visible spectrophotometry. The uncertainties on the $\delta^{18}O$ and δD values are ±0.05‰ and ±1‰, respectively.

Results of water analyses are given in Table 2. Also reported in Table 2 is the charge unbalance, which resulted to be lower than 3% for all the samples.

Table 1 – Physico-chemical parameters measured in the field

#	Location	Date	X UTM WGS84	Y UTM WGS84	Altitude (m.a.s.l.)	Flow rate (L/sec.)	T °C	pH	Elect. Cond. µS/cm	Total alkalinity (meq/L)
SO1	Laguna Socompa	20/04/2018	579923	7286205	3570	30-40*	24.9	7.48	1034	2.77
SO2	Laguna Socompa	20/04/2018	579961	7286189	3570	10	25.7	7.46	863	2.46
SO3	Laguna Socompa	20/04/2018	579872	7286263	3570	-	25.5	8.63	20400	8.30
SO4	Laguna Socompa	20/04/2018	579871	7286260	3566	-	25.5	7.40	1120	3.05
SO5	Laguna Socompa	20/04/2018	579876	7286264	3568	-	22.7	8.18	98700	15.0
SO6	Laguna Socompa	20/04/2018	579760	7286368	3570	0.0075	21.6	7.58	1753	2.67
SO7	Laguna Socompa	20/04/2018	579803	7286334	3572	-	16	7.59	1769	4.15
SO8	Laguna Socompa	21/04/2018	579596	7286667	3573	-	9.2	7.65	1701	2.52
SO9	Laguna Socompa	21/04/2018	580925	7286679	3564	-	10.2	7.06	306	1.50
SO10	Laguna Socompa	21/04/2018	580040	7286149	3565	0.1	19.7	7.55	907	2.95
SO11	Quebrada del agua	21/04/2018	585118	7288593	3850	0.55	18	7.32	109	0.63
SO11bis	Quebrada del agua	21/04/2018	584903	7288778	3810	-	16.8	n.m.	110	n.m.
SO12	Quebrada del agua	21/04/2018	584861	7288822	3800	-	14.6	n.m.	n.m.	1.80
LL1	Lullaiaco	22/04/2018	574416	7263007	3765	30	18.2	7.90	22800	1.60
LL2	Lullaiaco	22/04/2018	574482	7262869	3765	-	16	7.88	30300	1.40
LL3	Lullaiaco	23/04/2018	566057	7255160	3765	0.5	26.5	7.46	14130	2.03
LL4	Lullaiaco	23/04/2018	565931	7254843	3774	-	14.5	7.90	13000	2.51
LL5	Lullaiaco	23/04/2018	565532	7254773	3791	-	29.6	7.51	27500	1.89
LL6	Lullaiaco	23/04/2018	565839	7256080	3765	5-10*	26	7.44	18000	3.49
LL7	Lullaiaco	23/04/2018	567553	7249787	3765	3-4*	21.2	7.67	10800	2.38
SO13	Lullaiaco	24/04/2018	594789	7263098	4271	1.5	11.5	8.00	221	1.55
SO14	Chorillos?	24/04/2018	756825	7320057	4540	-	5.2	n.m.	n.m.	0.85
SO15	San Antonio de Los Cobres	25/04/2018	771756	7318829	3795	-	7.1	n.m.	435	n.m.
SO16	San Antonio de Los Cobres	25/04/2018	771327	7318540	3834	-	8	n.m.	303	1.80

n.m. – not measured

* - Estimated values

Table 2 - Chemical and isotopic composition of water samples from the Socompa Geothermal Prospect.

All chemical concentrations of major and minor components are expressed in mg/L, whereas the isotopic composition of oxygen and deuterium are referred to V-SMOW.

#	Na	K	Ca	Mg	Li	Cl	NO_3	SO_4	HCO_3	SiO_2	B	Sr	F	Br	NH_4	$\delta^{18}O‰$	δD‰	Charge Unbalance %
SO1	100	10.4	57.5	21	0.3	130	5.6	117	169	61.6	2.58	0.31	0.27	<0.2	<0.1	-9.34	-76.21	1.7475
SO2	81.3	10.6	43.4	19.4	0.27	97.3	6.4	104	151	65.9	2.38	0.27	0.27	<0.2	<0.1	-9.32	-76.8	0.9237
SO3	8471	1168	130	820	24.1	9176	<0.2	9850	506	85.6	117	1.1	1.47	9.6	0.2	-5.87	-59.14	0.3785
SO4	101	12.2	67.7	24.8	0.32	137	5.7	137	186	63.8	3.02	0.34	0.25	0.14	<0.1	-9.3	-76.34	1.6356
SO5	37200	5010	318	3042	88.7	40094	<0.1	42305	914	101	444	3.26	3.92	28.9	0.71	0.32	-28.86	-0.038
SO6	213	33.9	84.7	31.4	0.35	281	5.9	292	163	63.7	3.9	0.43	0.29	0.51	<0.1	-9.49	-78.71	0.7488
SO7	203	19	98.1	34.5	0.41	230	<0.1	267	253	34	4.43	0.54	0.31	0.47	n.a.	-9.5	-77.92	2.8315
SO8	220.3	37.3	83.8	28.6	0.37	285	<0.1	295	154	66.3	3.56	0.42	0.35	0.27	<0.1	-9.52	-77.59	1.3193
SO9	30.8	4.63	22	4.11	0.05	26.6	2.6	31.4	91.7	57.7	0.45	0.11	0.3	<0.2	n.a.	-8.89	-76.15	-0.6914
SO10	81.2	11.5	58.5	21.7	0.29	113	4.4	114	180	73.6	2.63	0.31	0.31	<0.2	<0.1	-9.19	-75.98	0.0139
SO11	13.6	1.3	4.53	2.13	0.02	2.57	3.93	11	38.5	63.7	0.22	0.03	0.25	<0.2	<0.1	-8.81	-71.13	1.7940
SO11_bis	n.a.	n.a.	n.a.	n.a.	n.a.	n.a.	n.a.	n.a.	n.a.	n.a.	n.a.	n.a.	n.a.	n.a.	n.a.	-8.74	-71.04	-
SO12	23.2	8.7	7.8	3.5	0.04	5.5	<0.1	3.92	110	50	0.32	0.06	0.36	<0.2	n.a.	-8.34	-68.93	-2.9843
LL1	5507	593	112.3	232	16.9	9286	<0.5	971	97.6	66.7	26	0.87	0.72	<0.2	<0.1	-8.53	-72.55	-0.3253
LL2	6097	557	92.5	262	19.7	10718	<0.5	1030	85.4	41.3	36.4	0.74	<0.2	<0.2	n.a.	-8.69	-74.24	-2.6265
LL3	2772	301	218.4	121	8.82	4727	<0.5	818	124	58.3	42.8	1.39	1.01	1.52	n.a.	-6.8	-63.45	-0.6318
LL4	2800	255	331	154	8.7	4760	<0.5	951	153	38	38.5	2.09	1.15	1.03	n.a.	-6.46	-62.91	0.7354
LL5	5805	649	217	228	18.7	9800	<0.5	995	115	75.4	40.9	1.42	0.91	2.01	n.a.	-6.39	-61.97	0.4089
LL6	3752	438	296	216	13.1	6580	<0.5	876	213	90.9	39.9	2.28	0.98	2.22	<0.1	-6.7	-63.4	0.3966
LL7	2166	257	83.2	109	6.38	3481	<0.5	695	145	83.4	10.3	0.44	0.86	<0.2	<0.1	-7.83	-68.5	-0.0756
SO13	13.6	3.3	23	3.6	0.01	10.4	1.5	18	94.7	41.3	0.33	0.12	0.28	<0.2	n.a.	-8.3	-68.76	-2.6519
SO14	11.1	4.94	36.4	7.77	<0.01	16.5	0.8	75.9	51.9	n.a.	0.83	0.26	0.2	<0.2	n.a.	-11.38	-81.35	2.8647
SO15	n.a.	n.a.	n.a.	n.a.	n.a.	n.a.	n.a.	n.a.	n.a.	n.a.	n.a.	n.a.	n.a.	n.a.	n.a.	-9.58	-69.78	-
SO16	40.0	3.76	20.0	4.04	0.18	20.5	<0.1	32	110	15	0.84	0.19	0.6	<0.2	n.a.	-11.39	-79.79	2.5421

n.a. - not analysed

3. Thermal manifestations

Thermal springs in the SGP are mostly distributed around the Socompa lagoon, near to the Socompa volcanic complex, at elevations close to 3600 m.a.s.l. (Figure A4). The only exception is represented by the thermal springs of the Quebrada del Agua, which are situated about 4km to the east of the Socompa lagoon. At 25Km south to the Socompa lagoon, there is another well-known thermal sector located at the Llullaillaco salar (Figure A5).

Socompa lagoon. Solid products directly originated by hydrothermal activity are present in the Socompa lagoon. Horizontal layers of white diatomite characterize a large parts of the Socompa lagoon border, together with sodium sulphate deposits. Thermal waters, with maximum temperature close to 26°C, discharges from the rock formation very close to the shore of the lagoon. Several seeps are also present and the mixing with the salty water from the lagoon influences them. All thermal springs are located to the south-west and west side of the lagoon (Fig.A4). Flow rate measurement for samples SO1 and SO2 are 35 and 10 L/sec, respectively. It is difficult to establish the overall flow rate of thermal waters, also because some springs discharge water at the bottom of the lagoon. Sample SO10 represents thermal water discharging from spring located inside a vegetated area. It was impossible to reach the discharge point and therefore its temperature (20°C) was certainty influenced by cooling (air temperature 12°C).

Quebrada del Agua. Quebrada del Agua spring is located at the river mouth, entering in the Socompa lagoon plain (Fig.A4). This spring is known as thermal since its temperature is 18°C, higher than the mean annual temperature (-5°C; Houston J and Hartley A.J., 2003). The flow rate is estimated in 0.6 L/sec. at the exit point of the SO11 sample, but various discharge points are present. Also, a pipe distributing the water from the spring location to the mill of the old mine, close to the railway, is present. Flow rate of the pipe is 1.8 L/sec., but several water leaks were identified. Water discharging from the Quebrada del Agua spring seeps below the embankment of the railway and emerges to the opposite side, in which a small river is organized flowing towards the Socompa lagoon. The salinity of the water is very low (T.D.S.=141 mg/L).

Llullalliaco salar. This represents a natural flat expanses of ground covered by salt deposits located at about 25Km south-east of the Llullaillaco volcano. Salt deposits are rich in potassium, boron and lithium. At the western and south-western shores the are some thermal springs with maximum temperature close to 26°C. It is worth to mention that a temperature of 29.6°C was measured inside an old piezometer located at the western side of the salar (sample LL5) and various springs and seeps are also located to the eastern side with temperature 16-18°C

(which are anomalous taking into account the mean local air temperature). All collected water around the Llullaillaco salar show a very high salinity, reaching a maximum value >17000 mg/L (as T.D.S.). Just in a few points the flow rate was measured and in particular values of 30, 8 and 4 L/sec were estimated respectively for LL1, LL6 and LL7 springs.

4. Water chemistry

4.1 Hydrochemical classification

Water chemistry is initially analyzed in terms of the relative concentrations of major anions (HCO_3, SO_4, and Cl) and major cations (Na, K, Ca, and Mg) by means of the conventional Langelier-Ludwig (LL) compositional pyramid and relevant cross-section (Langelier and Ludwig, 1942; Tonani, 1982). In the LL compositional diagrams the samples are displayed using a suitable coefficients R_i, calculated starting from the concentrations (C_i) expressed in eq/L:

$$R(Na+K) = 50 * \frac{(C_{Na} + C_K)}{(C_{Na} + C_K + C_{Ca} + C_{Mg})}$$

$$R(Ca+Mg) = 50 * \frac{(C_{Ca} + C_{Mg})}{(C_{Na} + C_K + C_{Ca} + C_{Mg})}$$

$$R(HCO3) = 50 * \frac{(C_{HCO3})}{(C_{HCO3} + C_{Cl} + C_{SO4})}$$

$$R(HCO3+SO4) = 50 * \frac{(C_{HCO3} + C_{SO4})}{(C_{HCO3} + C_{Cl} + C_{SO4})}$$

$$R(HCO3+Cl) = 50 * \frac{(C_{HCO3} + C_{Cl})}{(C_{HCO3} + C_{Cl} + C_{SO4})}$$

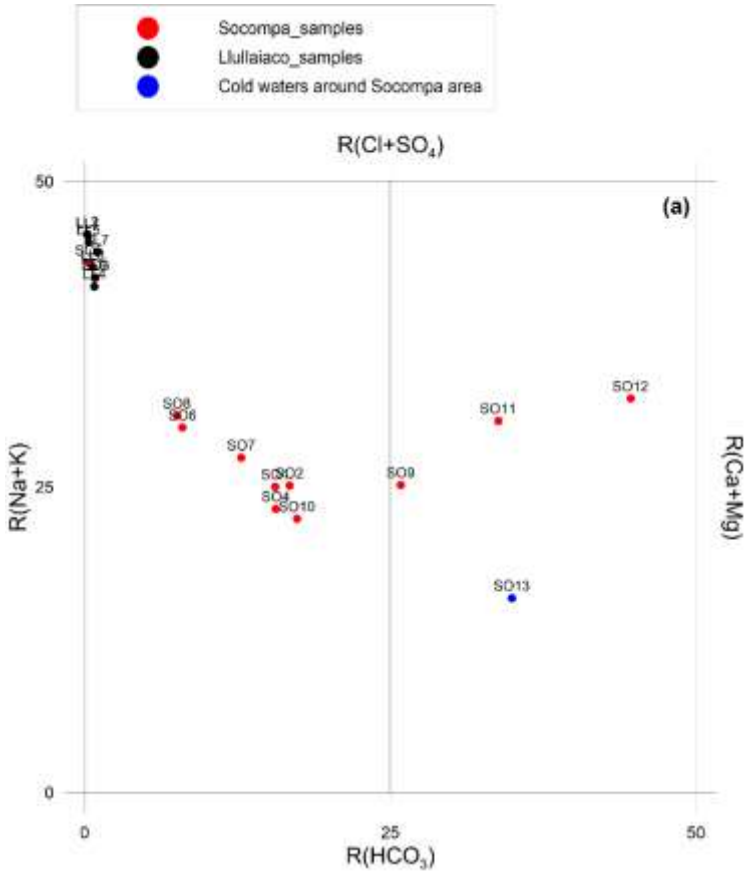

Figure 1a. LLHCO3 diagram for waters collected in the Socompa Geothermal Prospect.

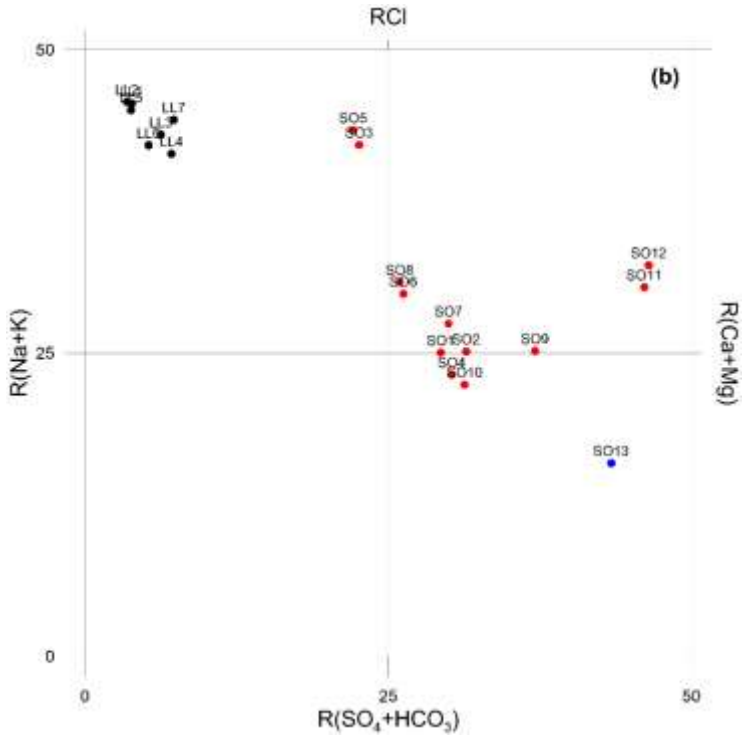

Figure 1b. LLCl diagram for waters collected in the Socompa Geothermal Prospect. Symbols as in figure 1a

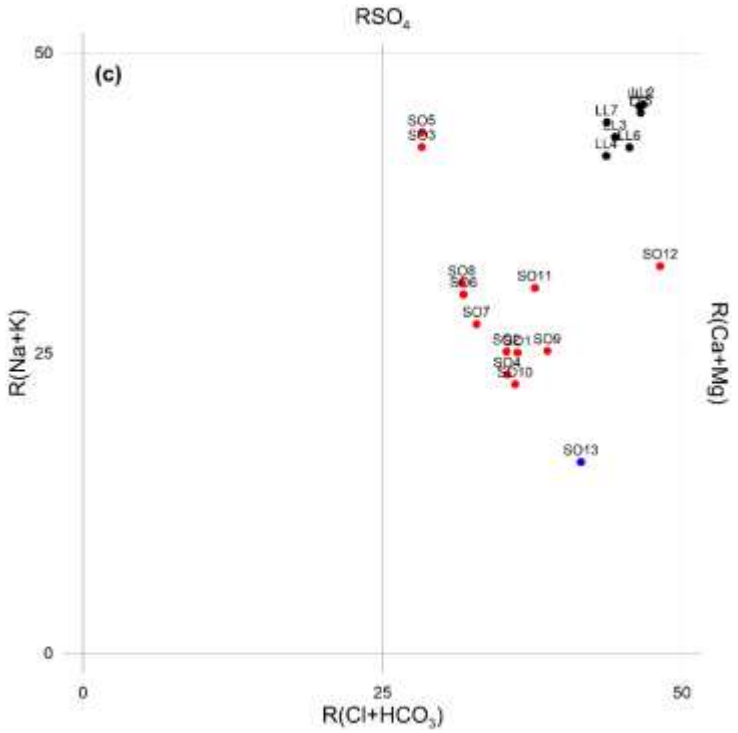

Figure 1c. LLSO4 diagram for waters collected in the Socompa Geothermal Prospect. Symbols as in figure 1a

Figures 1a, 1b and 1c show that all waters collected around the Llullaillaco salar are Na-Cl rich. Cold water SO13 are $CaHCO_3$-rich. Thermal waters located close to the Socompa lagoon (SO1, SO2, SO4 and SO10) show mixed composition, having similar concentrations of Cl, SO_4 and HCO_3. Although the sample from Quebrada del Agua (SO11) has a temperature of 18.0°C (not properly low considering the altitude) it shows a different chemical composition, belonging to the "HCO_3-rich waters type". Similar characteristics are shown by samples SO12 (also located in Quebrada del Agua area), representing water coming from wet soil characterized by the presents of local vegetation (i.e. Vega). Samples SO5 (collected directly from the Socompa lagoon) and SO3 are Cl-SO_4 rich-water and show a different chemical composition from the Llullaillaco springs (are also affected by the presents of salt depositions/formations). Sample SO9, a cold spring (10.2°C) located close to the rim of the Socompa lagoon, seems not to be affected by the present of salt depositions/formations and/or salty water from the Socompa lagoon. On the contrary, samples SO6, SO7 and SO8 seems affected by salt or salty waters since in the LL diagrams they are shifted towards salty waters, as SO3 or SO5. More in general, the LL diagrams show different chemical compositions for sampled "thermal waters" compared to the others samples, suggesting different origin and/or evolution trends. In figure 2, in which iso-

ionic salinity lines are reported, collected waters show big differences in total salinity, ranging between 2 and 4000 meq/L. The lowest value is that of sample SO11, the known thermal water of Quebrada del Agua, whereas the highest value characterize the sample SO5 (water of the Socompa lagoon). Sample SO3 clearly represents a mixing between water from the Socompa lagoon and water characterized by much lower salinity. The rest of cold and thermal waters collected in the SGP (SO1, SO2, SO4, SO6, SO7, SO8, SO9 and SO10) exhibit low values of total salinity (see figure 2b), ranging from 6 meq/L (SO9), 13-20 meq/L (SO1, SO2, SO4 and SO10) and 33 meq/L (SO6, SO7 and SO8). All samples from Llullaillaco show a very good alignment, suggesting a mixing line connecting the more and the less salty samples collected, respectively LL2 (TDS ≈ 640 meq/L) and LL7 (TDS ≈ 240 meq/L). It is worth to mention that this alignment is clearly separated by that involving the water from the Socompa lagoon (SO5). This feature suggests a probably different origin and evolution of fluids.

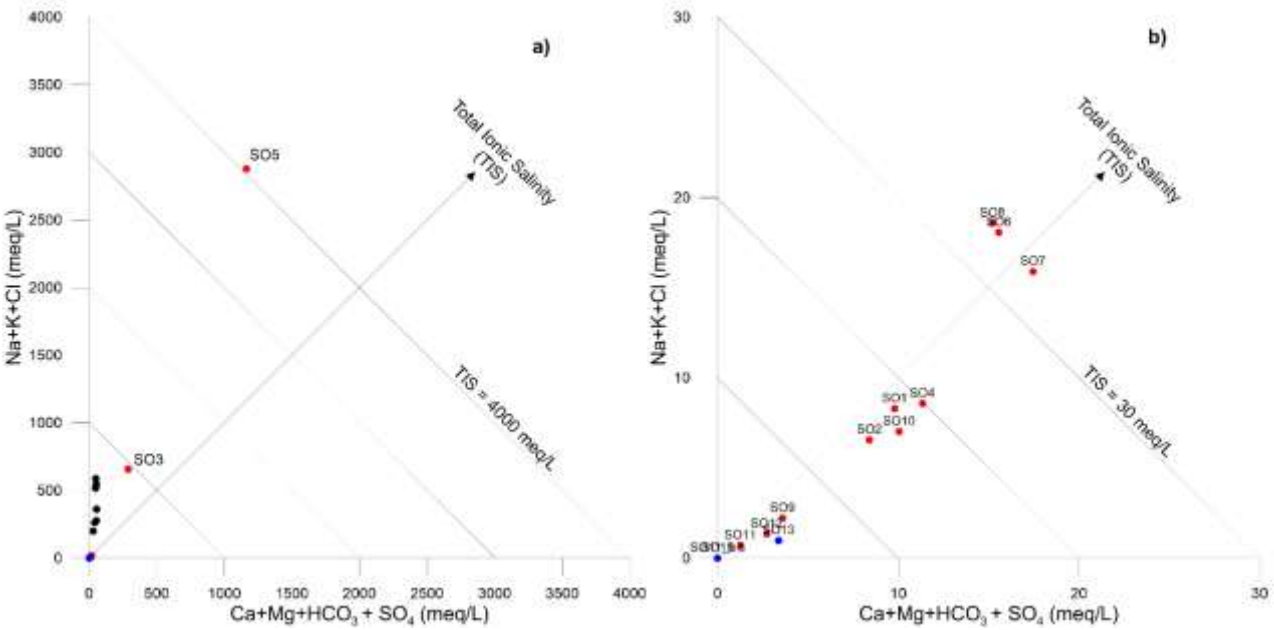

Figure 2. a) Triangular cross section of the LL compositional diagram. The lines represent iso-salinity values. Symbols as in figure 1a. **b)** Enlargement of previous diagram, for salinity values up to 30 meq/L.

4.2 Chloride plots

In this section, each chemical constituent is plotted against chloride, chosen as reference component owing to its mobile behavior, unless saturation with halite is attained, which is not the case for any of the considered waters. These chloride plots are useful to investigate both the behavior of the analyzed chemical constituents and the relationships among the water samples collected in the SGP, which is essential for individuating active processes (e.g., mixing,

separation of solid phases, etc.). This is also a necessary propaedeutic step before tackling chemical geothermometry.

The influence of salt deposits/formations and or salty water is evident in all binary plots (Fig.3a-f), in which, as for reference, the "conservative mixing line" between the water of the Socompa lagoon (SO5) and a mean chemical composition of the local thermal component calculated starting from those of four main thermal waters (SO1, SO2, SO4 and SO10) discharging into the lagoon is reported. As shown by all chloride plots, SO3 represents a mixing between water of the Socompa lagoon and a more dilute water, similar to more thermal end-member identified (as samples SO1, SO2, SO4 and SO10). Samples SO6, SO7 and SO8 are distributed close to the mixing line, suggesting also for these waters an interaction/dissolution of salts and/or mixing with salty water (as SO5). However, their stable isotopes show a more depleted composition compared to the "thermal waters" SO1, SO2, SO4 and SO10 (see Fig.3g and h), suggesting a possible different fresh water end-member (higher infiltration altitude) or a quite more complicated physico-chemical processes actives in the feeding zones (i.e. melting of ice cap, refreezing, ecc). The influence of salt depositions/incrustations is suggested also by the observation of the geological map (Zappettini and Blanco, 2001) in which various geological formations containing gypsum, limestone and halite are documented. These lithologies are also well-known in the study area and abroad (Ramirez, 1998).

The most thermal waters identified in the SGP are represented by samples SO1, SO2, SO4, SO10 and SO11, even if they show a low TDS values (dilute waters). Salt depositions/formations or salty waters are extensively present in and around the SGP and in such conditions the pristine chemical characteristics of circulating waters (deep thermal end-member but also fresh components) can be modified, making it difficult the study of the evolution of thermal deep components. This occurrence is shown in chloride plots of figures 3 a-h, in which it is not possible to identify a clear "geochemical evolution trend" for the thermal waters SO1, SO2, SO4, SO10 and SO11 (i.e. mixing line connecting dilute cold waters with thermal end-members). Cold water SO8 has TDS values very close to that of thermal waters, highlighting the role of salt deposits. This situation seems to characterize also the Llullaillaco salar in which the more thermal waters (LL3, LL5, LL6 and LL7) have TDS values less than the values of others waters.

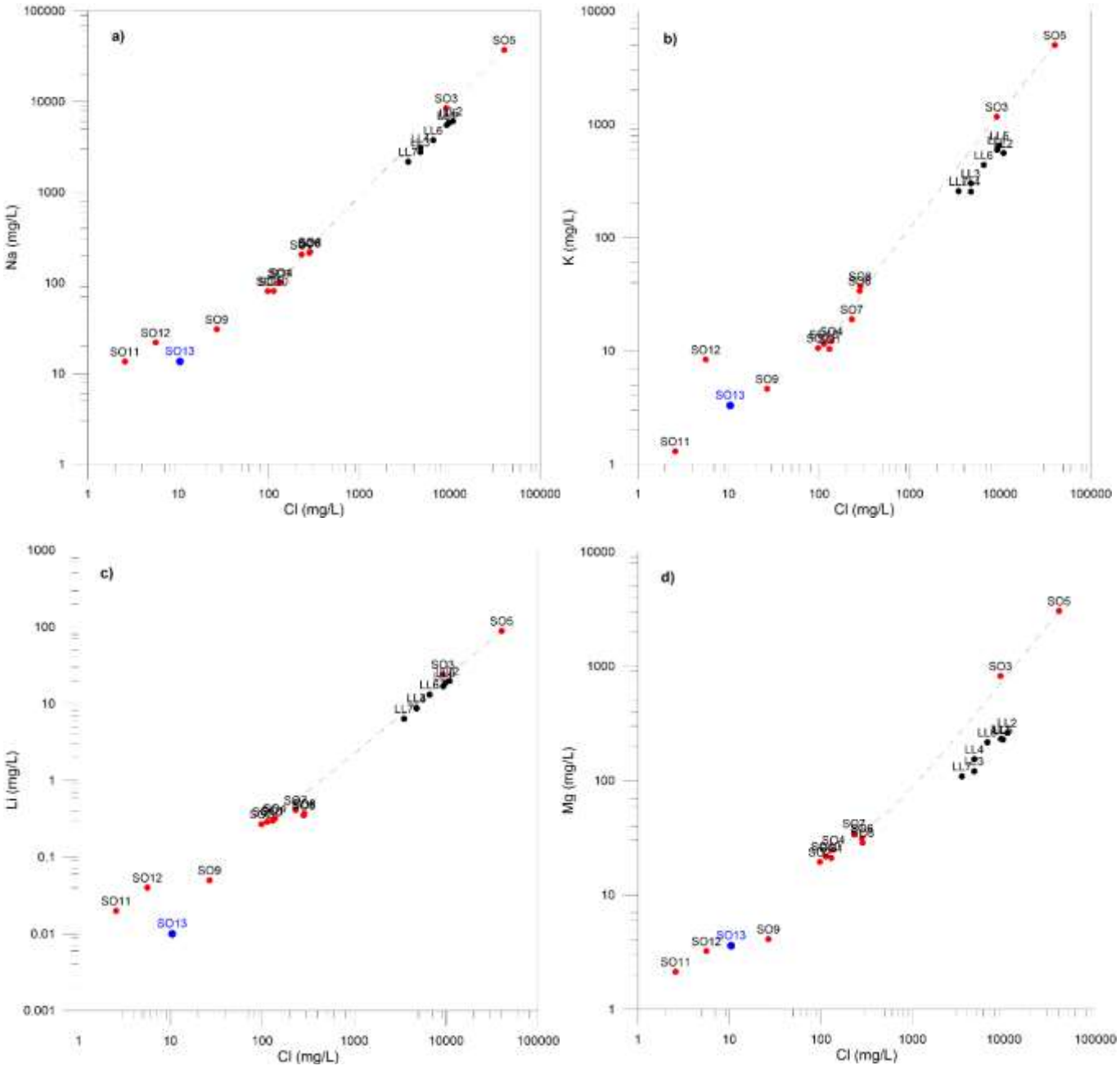
a)
Na (mg/L)
Cl (mg/L)
SO5
SO3
SO6
SO9
SO12
SO11
SO13
b)
K (mg/L)
Cl (mg/L)
SO5
SO3
SO7
SO12
SO9
SO13
SO11
c)
Li (mg/L)
Cl (mg/L)
SO6
SO12
SO9
SO11
SO13
d)
Mg (mg/L)
Cl (mg/L)
SO5
SO3
SO9
SO12
SO13
SO11

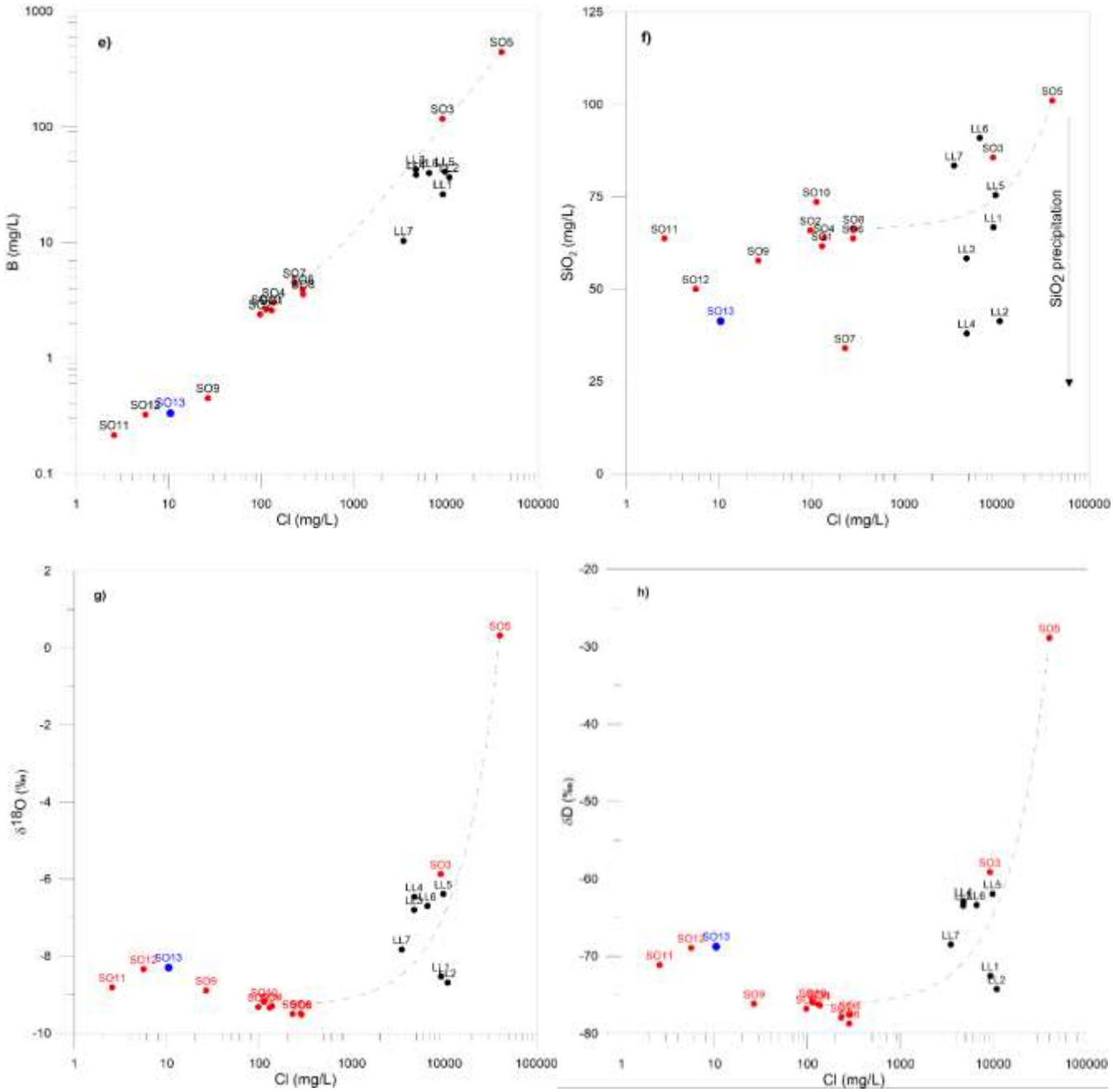

Figure 3. Plots of chloride content vs the content of a) sodium, b) potassium, c) lithium, d) magnesium, e) boron, f) silica, g) 18-oxygen and h) deuterium. Symbols as in figure 1a. The dashed line represents the evolution of chemical composition expected for mixing between water from the Socompa lagoon (SO5) and thermal waters (calculated as mean value of SO1, SO2, SO4 and SO10 thermal samples).

In figure 3f (SiO_2 vs Cl) the scattering of points could be due to precipitation of silica which can be occur very fast close to the discharge point of thermal and no thermal springs. In fact, rocks present in the studied area are silica-rich, being represented by volcanic products most of these are composed by volcanic glass. Circulating waters (including cold waters) can dissolve high content of silica from rocks and oversaturation conditions of silica polymorph (i.e.

amorphous silica, opal or β-cristobalite, chalcedony) can be reached. This is a relatively rapid process upon attainment of saturation with respect to this mineral phases, triggered by conductive cooling of thermal waters. In fact most thermal waters plot close to the solubility curve of opal in the correlation plot of silica vs. temperature (Figure 4), corroborating this hypothesis.

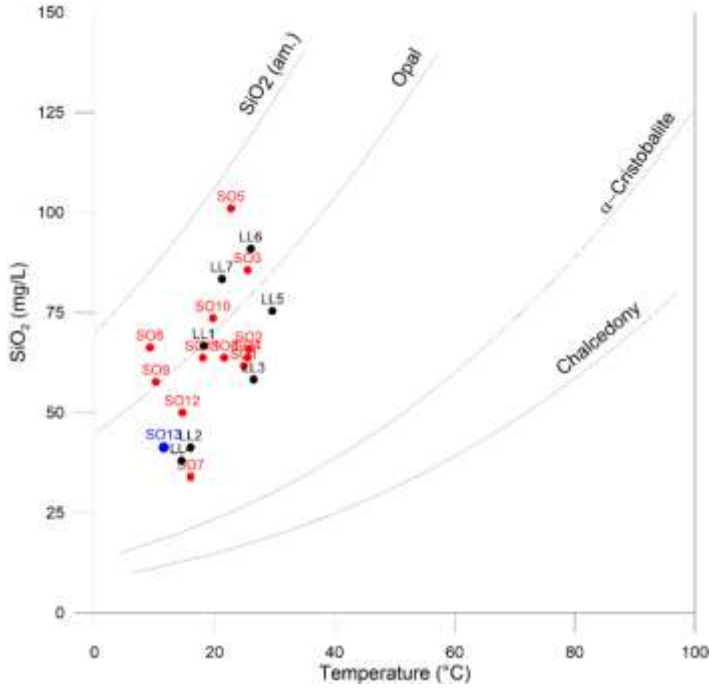

Figure 4. Binary plot SiO_2 vs Temperature. Symbols as in figure 1a

Some water samples from Llullaillaco salar show higher Ca, Sr and SO_4 contents compared to waters collected in the SGP, as shown by figure 5 a, b and c. This is probably due to the interaction with different geological formations and/or mineralizations, rich in these chemical components. This condition is supported by the geological map (see Fig.3Ab – Zappettini and Blasco, 2001) in which samples LL3, LL4, LL5, LL6 and LL7 are located on the west side of the Llullaillaco salar characterized by the presence of different geological formations compared to those outcropping on the east side. It is interesting to note that springs LL are all located on the trace, or very close to it, of regional faults (see Fig.A6). However, the scatter of points in figure 5a, 5b, 5c and 5d can be also explained in terms of a re-equilibration processes, like calcite precipitation, as shown by figure 5a, 5b and 5d. This hypothesis seems to be confirmed by the values of calcite Saturation Index (SI - calculated using the EQ3NR software package – Wolery and Jarek, 2003) for samples LL1 (-0.22) and LL4 (0.48). Values of the SI_i close to 0, <0 or >0, respectively define conditions close, under or over the saturation of a generic mineral phase i.

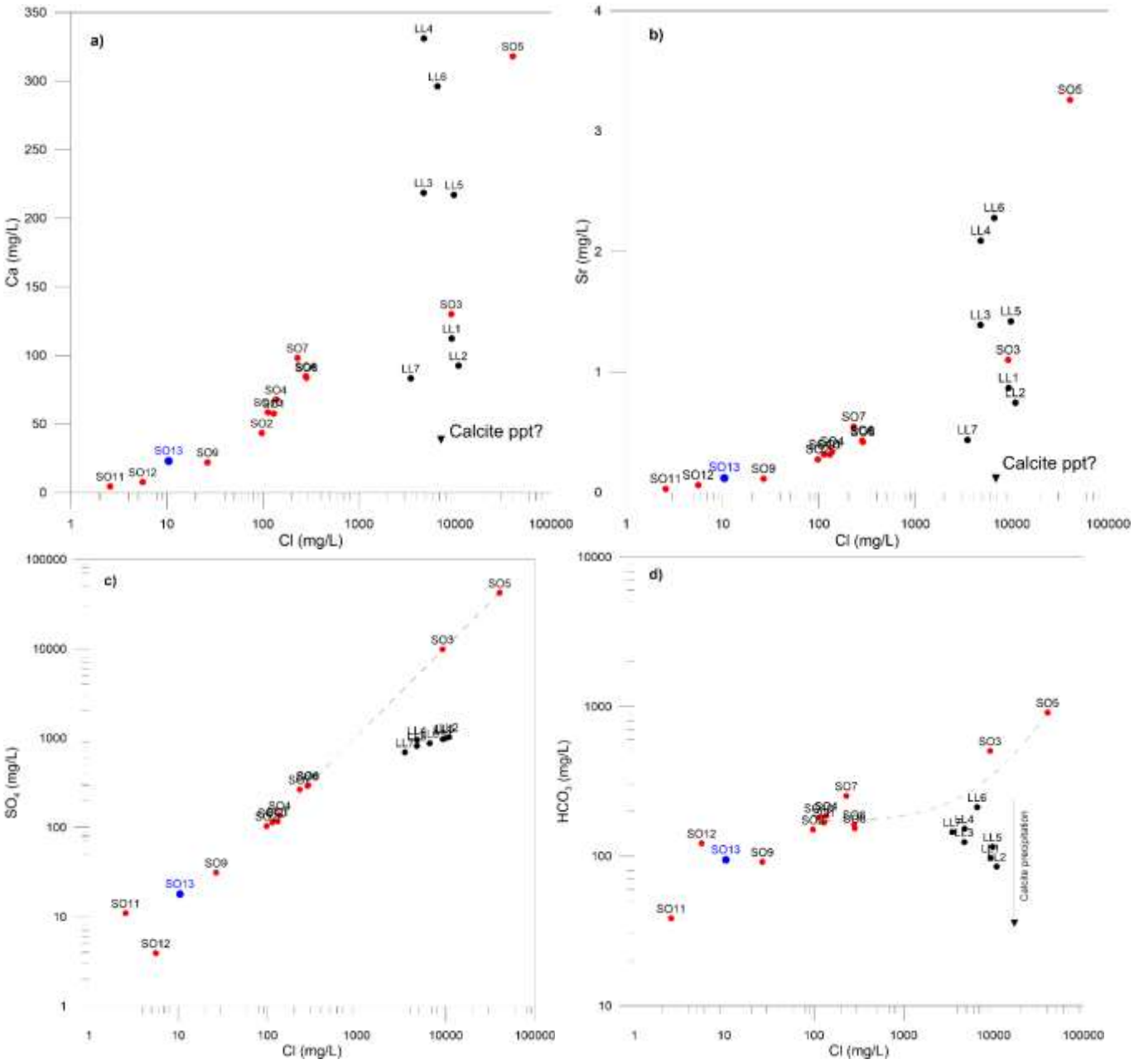

Figure 5. Plots of chloride content vs the content of a) calcium, b) strontium, c) sulfate, d) bicarbonate. Symbols as in figure 1a.

4.3 Geothermometry

As suggested by Giggenbach (1986, 1988), there are several graphical techniques able to identify waters that have attained full equilibrium conditions (at P_{CO2}, T conditions fixed by univariant reaction involving calcite, calcium-aluminium silicate, K-feldspar, muscovite and chalcedony – Giggenbach, 1984, 1986, 1988) with thermodynamically stable mineral

assemblage from less evolved immature waters. However, geochemical exploration studies performed in many explored geothermal systems have shown that secondary processes active during the rise of a deep geothermal component, such as mineral phase separation, leaching and dissolution, vapor loss or vapor gain, dilution and mixing, are able to limit the applicability of geothermometric techniques.

Based on this statement and on the discussion of the previous section, there seem to be little hope to obtain meaningful evaluations of temperatures present in deep circuits through the application of geothermometric functions.

Bearing in mind these difficulties, it is useful to inspect three powerful graphical tools proposed by Giggenbach and coworkers (Giggenbach, 1988; Giggenbach et al., 1994).

Two of these graphical tools, namely the triangular diagram of Na-K-$Mg^{1/2}$ and the correlation plot of Mg/(Mg+Ca) vs. K/(K+Na) are shown in Figures 6a, 6b and 7. In all graphs, the analytical data of samples collected during this study are compared with:

(i) the aqueous solution in full equilibrium with the secondary hydrothermal minerals formed through iso-chemical recrystallization of an average crustal rock, at different reservoir temperatures;

(ii) the aqueous solution compositions expected through dissolution of granite, basalt and an average crustal rock.

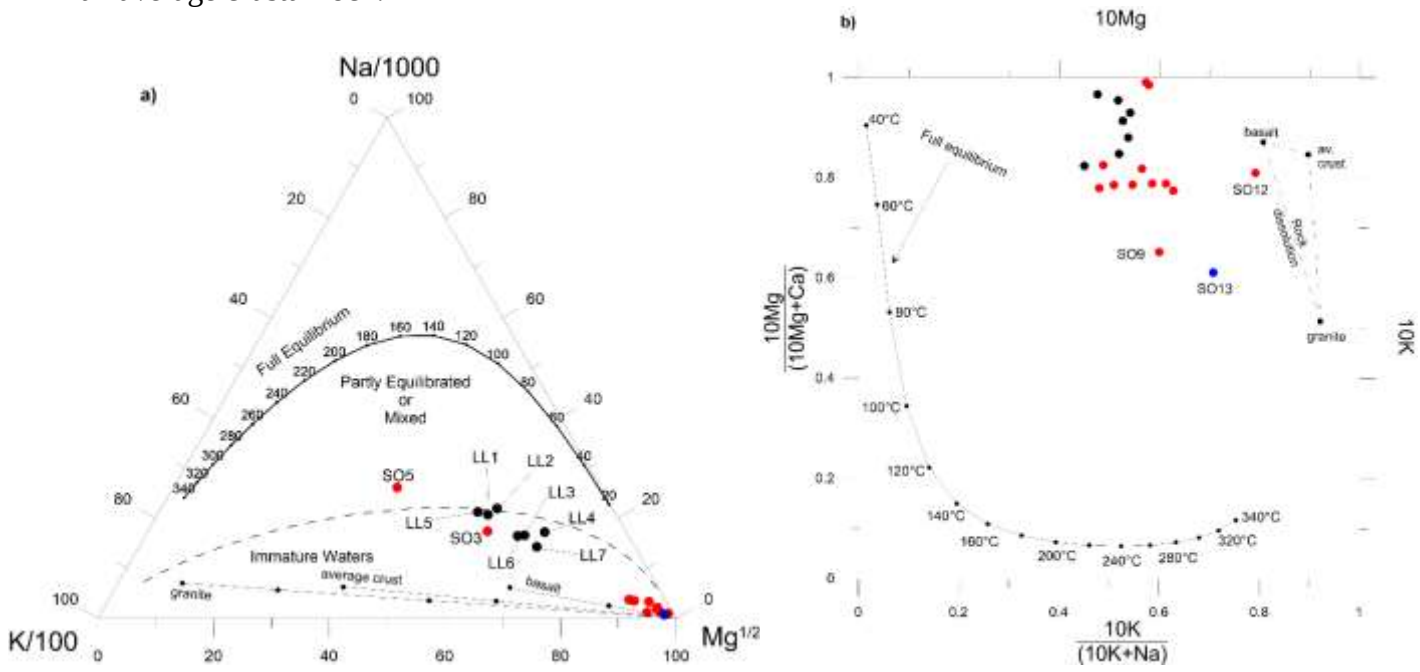

Figure 6. (a) Triangular diagram of Na-K-$Mg^{1/2}$ and (b) correlation plot of 10 Mg/(10 Mg + Ca) vs. 10 K/(10 K + Na). In both graphs analytical data are compared with the condition of full equilibrium between the aqueous solution and the secondary hydrothermal minerals formed through iso-chemical recrystallization of an average crustal rock as well as the compositions expected through dissolution of granite, basalt and an average crustal rock (from Giggenbach, 1988). Symbols as in figure 1a.

In Figure 6a, all the thermal waters (SO1, SO2, SO4, SO10, LL3, LL5 and LL6) are found in the field of the so-called immature waters, either close to the $Mg^{1/2}$ –vertex, where the cold waters are positioned. This spread of points confirms the relative enrichment in Mg, which can be due to either addition of cold shallow waters or preferential Mg acquisition upon cooling or both processes. It is worth to mention that the shifting towards the full equilibrium line regard just the waters characterized by high TDS values. Therefore, it seems to be governed by salt dissolution or mixing with salty waters (as SO5) and not by full equilibrium between the aqueous solution and the secondary hydrothermal minerals formed through iso-chemical recrystallization of an average crustal rock.

A similar picture is provided by Figure 6b, with all collected waters (independently from the salinity) distributed in the immature waters field. Only cold waters SO9 and SO13 are displaced towards the full equilibrium line, but such a displacement is probably due to acquisition not only of Mg but also of Ca.

For what discussed in the previous section regarding the pivotal role of a) salts deposits (that are Na-Cl-SO_4 rich), b) mixing with salty waters and also c) dilution with fresh surface waters, the temperature estimations performed using the Na-K and Na-K-Ca functions are questionable.

Figure 7 presents another useful graphical technique, which is obtained combining the two chemical subsystems responding most rapidly to changes in temperatures, that is those based on dissolved silica and on the K^2/Mg ratio (Giggenbach, et al., 1994). All thermal waters of the SGP (SO1, SO2, SO4 and SO10) plot half-way between the full equilibrium lines (labeled conductive cooling and adiabatic cooling) and the amorphous silica line. This spread of points can be attributed to either (i) saturation with a silica polymorph of intermediate solubility (e.g. opal-CT as seen in the figure 4) or (ii) disequilibrium between the two considered chemical subsystems, owing to either dilution of thermal waters or preferential acquisition of Mg upon cooling or both processes, as already noted above. Waters characterized by high TDS values are distributed on the right of the full equilibrium line for conductive cooling. This is probably due to the interaction/dissolution of salts (the silica content of most salty waters is in the same order of magnitude of those for dilute waters, including thermal waters) and/or calcite precipitation. Also, the scatter of points towards less $Log_{(SiO2)}$ values is compatible with silica precipitation (as described in previous section).

Although there are no “mature waters” suitable for the application of geothermometers are present in the collected samples, we can try to obtain some temperature estimations from the most thermal waters, probably less affected by the presents of salts. As seen in the previous section, these samples are SO1, SO2, SO4 and SO10. The estimation considering $SiO_{2(am)}$ and

Opal are close to the temperature measured at the exit points (≈25-26°C - see Fig.4), as these samples are close to saturation with these mineral phases (especially Opal). Temperature estimation performed considering α-cristobalite or chalcedony reach maximum values around 70°C and 95°C, respectively (sample SO10 in fig.4). Taking into account the hydrogeochemical features of collected samples, the hypothesis of the equilibrium with quartz quenched at more high temperature is questionable.

Temperature estimations performed using K^2/Mg geothermometer give lower values (≈60°C). This is not surprising as K^2/Mg ratio re-equilibrates faster upon cooling (Giggenbach, 1986, 1988).

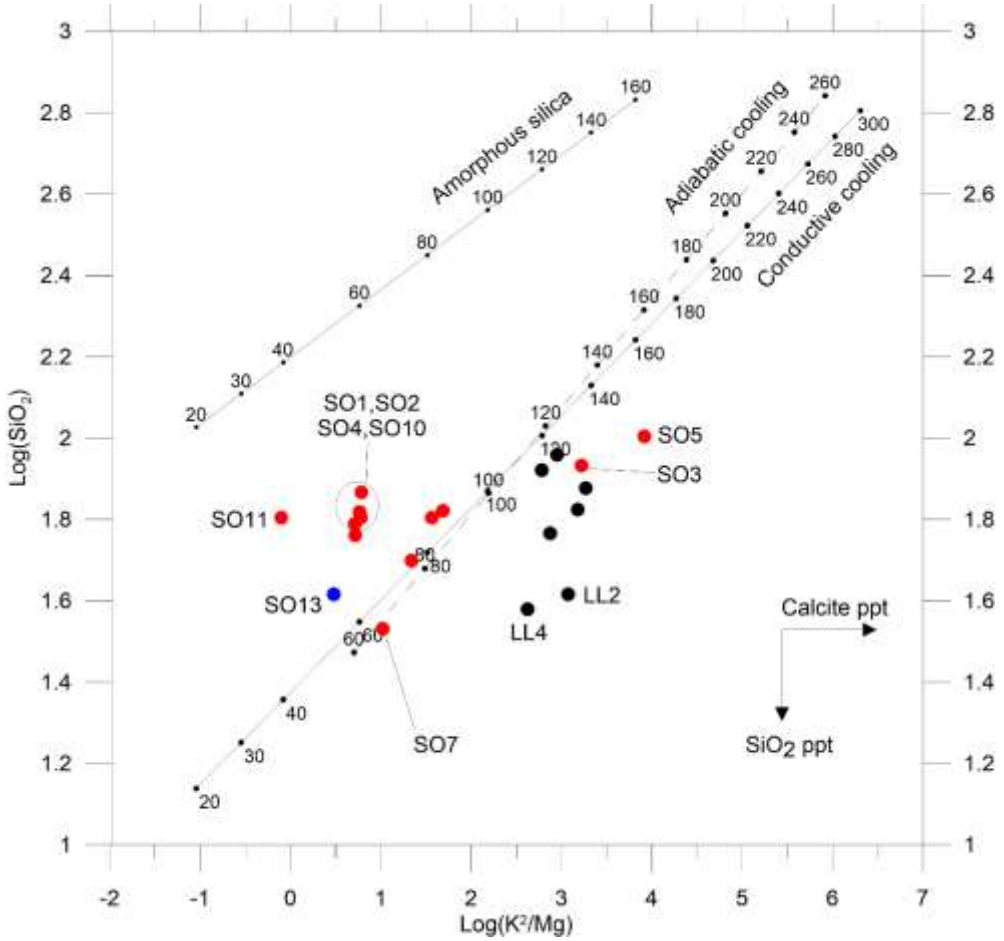

Figure 7. Plot of log(K^2/Mg) vs. log(SiO_2) (from Giggenbach et al., 1994) .

A different approach to chemical geothermometry is shown in Figgs.8a and 8b, where the changes in the saturation indexes (SI) of relevant minerals with temperature are shown for thermal springs, which have the highest outlet temperature discharging in the Socompa lagoon

(SO2 sample) and that of Quebrada del Agua (SO11 sample). These data were obtained by means of the EQ3/6 software package (Wolery, 1983; Wolery and Jarek, 2003). Obviously, the saturation indexes with respect to Opal approach zero around 25°C for both samples. Just for sample SO2, calcite crosses the opal SI vs T line close to the SI=0 at 38°C. It could suggest that this is the last equilibrium temperature reached by the water before the discharge even if a general disequilibium condition is shown by all mineral phases. Figure 8 also shows that these two springs are undersaturated with respect to gypsum and anidrite at any temperature between equilibrium and emergence values.

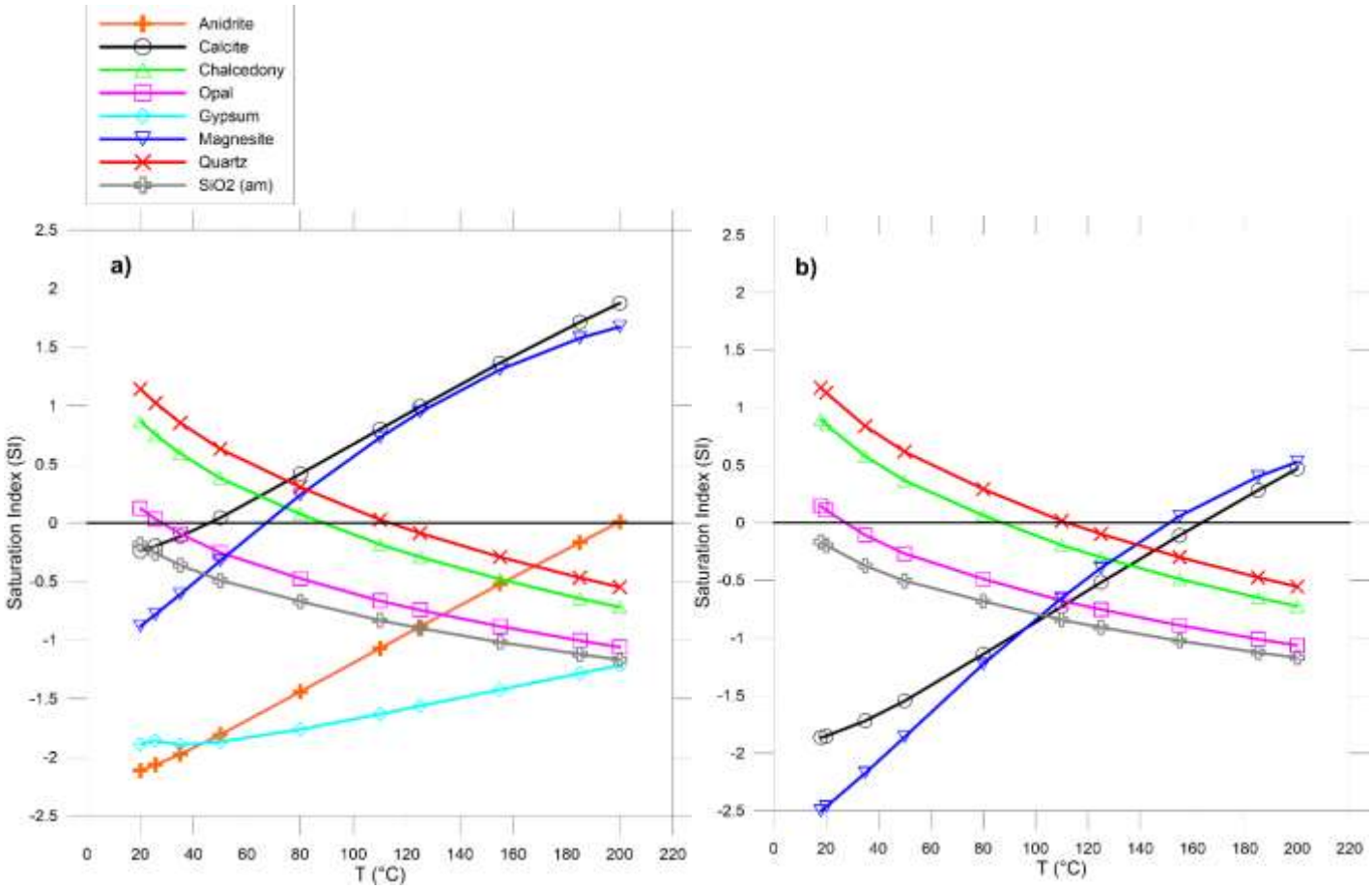

Figure 8. Evolution of saturation index (SI) as a function of temperature for a) SO2 and b) SO11 thermal springs.

5. Isotope geochemistry

In the elaboration of stable isotopes, data from local rain waters, snow, surface waters from snowmelt and wells collected to the west and north-west side of the Llullaillaco volcano (Alpers and Whittemore, 1990) were included in order to gain more information regarding possible feeding zone and the evolution of thermal fluids (see Fig.A1 for location). Samples from cold

springs collected in this study and located far from SGP and at different altitude were also considered (SO14, SO15, SO16).

In the classic correlation diagram $\delta^{18}O$ vs. δD values (Fig. 9), rainwaters plot on the Regional Meteoric Water Line (R.M.W.L. - $\delta D = 7.3 \cdot \delta^{18}O + 7.99$) determined by Fritz et al. (1978) for precipitation near the Salar de Atacama. The slope of this line is less than that of World Meteoric Water Line (W.M.W.L. - $\delta D = 8 \cdot \delta^{18}O + 10$), which is 8. Also, as suggested by Alper and Whittemore (1990), the "deuterium excess" for these rainwaters is greater than the global average values for precipitation (d = +10‰ – Yurtsever and Gat, 1981). These characteristics seems to be compatible with non-equilibrium evaporative effects (Gat and Carmi, 1970; Yurtsever and Gat, 1981) would contribute to the high deuterium excess in precipitation from hyper-arid Atacama region (Alpers and Whittemore, 1990).

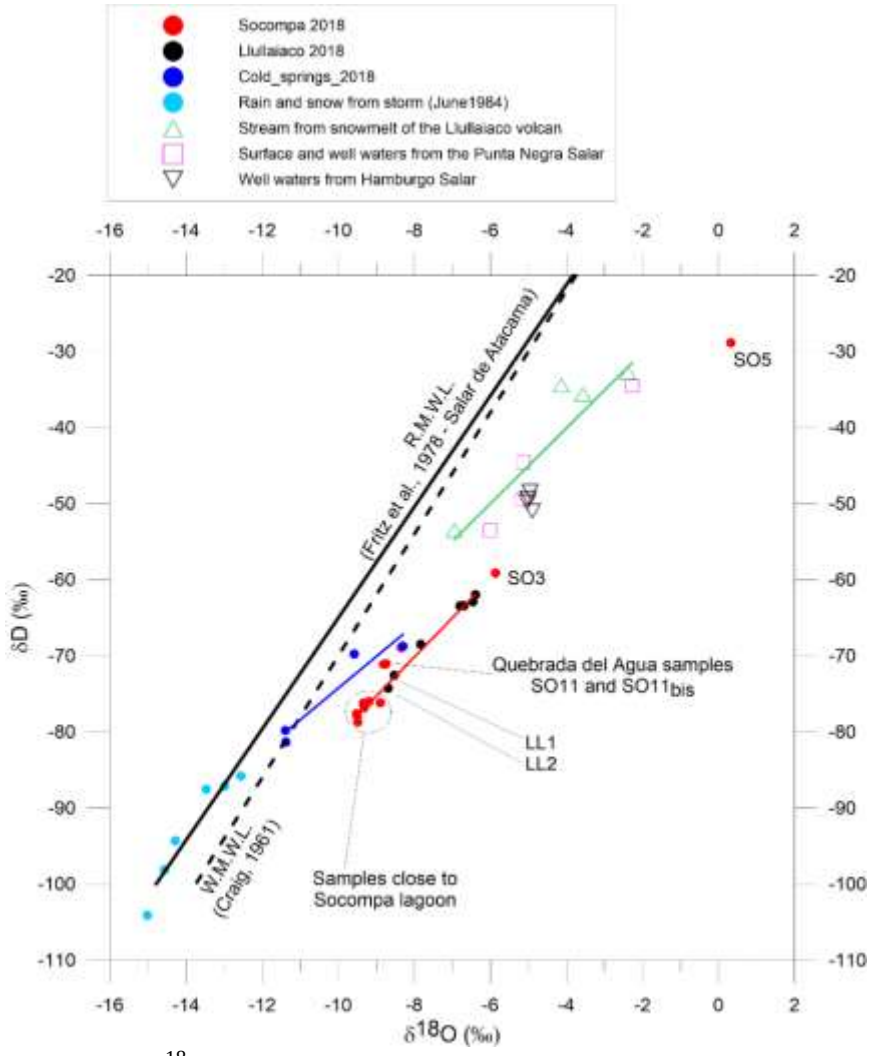

Figure 9. Correlation plot of $\delta^{18}O$ vs. δD values for waters collected in this study. The worldwide and regional meteoric water lines are also reported.

Cold waters collected during this study plot more close to the W.M.W.L., showing an alignment characterized by a slope of 4.16 (see blue line in figure 9). The difference between δD and $\delta^{18}O$ values of these springs probably reflect the difference in infiltration altitude: in fact the altitude of the springs differ a lot, ranging from 3795 and 4540 m.a.s.l. respectively for sample SO15 and SO14. However, more in general, others source of variations in isotopic compositions can be due to precipitation, evaporation and sublimation (Kendall and McDonnell, 1998). These processes are able to change, according to temperature, the stable isotopic composition of source water vapour and the surface characteristics that affect the energy balance and the evaporation/sublimation processes.

Cold and thermal waters discharging into the Socompa lagoon show similar stable isotopic compositions, suggesting similar feeding zone, even if the spring located on the south and south-east side of the lagoon (SO1, SO2, SO4, SO9 and SO10) have a slightly more heavy stable isotope composition compared to the others. Water from the lagoon (SO5) is an exception, being affected by heavy surface evaporation. Sample SO3, representing a mixing between water from the lagoon (SO5) and component similar to SO1, SO2, SO4 or SO10, is shifted towards SO5 sample following a simple mixing line (this feature is confirmed also by the diagrams $\delta^{18}O$ vs Cl and δD vs Cl, respectively Fig.3g and h). Thermal water collected in the Quebrada del Agua (SO11 and SO11bis) show a more enriched stable isotopic compositions suggesting different feeding zones and flow path compared to that for Socompa thermal springs. This hypothesis is also confirmed by its chemical characteristics showed by classification diagrams and chloride plots.

It is interesting to note that samples collected close to the Socompa lagoon and around the Llullaillaco salar define an alignment having a slope of 5.13 (red line in figure 9) which is very similar to the slope (4.97) for the alignment obtained for water from Punta Negra Basin (from Alpers and Whittemore, 1990 – see green line in figure 9). This could suggest a similar physical processes that affect the evolution of waters in this region. Even if the feeding zones can be similar, large differences in stable isotopic compositions can be appear in springs or rivers located in a closed basin sourced by snowmelt (as in various Regions located at high altitude in Andean's mountains). As melting season progress, due to the preferentially distribution of lighter isotopes (^{16}O and H) in liquid water, a depleted meltwaters and enriched remaining snowpack are initially generated. This process is analogue to fractionation during evaporation (Cooper et al., 1993; Rodhe, 1998; Taylor et al., 2001). Proceeding in melt season, meltwater became progressive less depleted and, conversely, the snowpack less enriched. This process, known as *isotopic elution* (Ohlanders et al., 2013), can be responsible for variations in isotopic composition up to 4-8 ‰ in $\delta^{18}O$ (Taylor et al., 2001; Unnikrishna et al., 2002; Cooper et al.,

1993). Isotopic elution, together with evaporation in hyper-arid region, could explain the large range of variation in stable isotopic composition of samples collected.

As for samples SO6, SO7 and SO8, feeding zones for samples LL1 and LL2 are probably located at higher altitude than the other samples collected around the Llullaillaco salar (see Fig.3g, 3h and Fig.9).

For what discussed before, the isotopic characteristics of thermal waters in the SGP seems to be ascribable to complex physical processes (i.e. various degrees of evaporation, sublimation, different altitude, isotopic elution), active immediately after the infiltration of the waters, and also to mixing with salty waters. Therefore, there is no apparent oxygen isotope shift. We recall that the shift in oxygen isotopes is a characteristic of many geothermal waters and may be due to either exchange of oxygen isotopes during high-temperature (>150°C) water-rock interaction or addition of andesitic (arc-type) magmatic water, which was originally defined by Giggenbach (1992a). However, the lack of oxygen shift is not necessarily a negative indication. In fact, dynamic, fluid-dominated systems (i.e., with high water/rock ratios) are characterized by relatively small oxygen isotope shifts, indicating adjustment of altered rock composition to water compositions (Giggenbach, 1991b). The opposite situation is found in essentially stagnant, rock-dominates systems which exhibit large oxygen isotope shifts, suggesting adjustment of water composition to unaltered rock compositions.

6. Final considerations

In the Socompa Geothermal Prospect (SGP, Salta Province - Argentina) an hydrogeochemical exploration study was performed in April 2018, 20^{th}-25^{th}. A total of 24 water samples were collected and in particular: 12 from thermal springs, 1 from thermal well located in the Salar of Llullaillaco, 1 from the Laguna Socompa, 6 from cold springs and 4 from salty springs located around it.

The SGP is located very close to the international border of Chile, between the Socompa lagoon and Socompa volcano, at an average altitude around 3500-3800 m.a.s.l. The Socompa volcano is a large composite volcano with an altitude of 6051 m.a.s.l., consisting of a central cone and several lava domes. Dacitic lava flows are also present. The last eruption is dated at about 7000 years BP (Ramirez, 1988), generating a pyroclastic surge deposits at Monturaqui (see location in Fig.A2). The basement below Socompa volcano is composed by Lower Paleozoic granitic and metamorphic rock, overlain by strata of the Devonian quartzities, Permian acidic volcanic rocks and Upper Cretaceous clays and sands of the Purilactus Formation (Reutter et al., 1994). Below the volcano there is a Miocene-Pliocene Salin Formation ≈200 m thick layer, capped only by Socompa-derived volcanoclastic layers (Ramirez, 1988 – see figA6 and A7). The thickness of this formation is also confirmed by drilling logs (Ramirez, 1988). The Salin Formation is mainly composed of gravels and conglomerates, poorly consolidated or unconsolidated, containing sand-rich layers up to 10m thick and hundreds of meters long. It is worth to mention that the Salin Formation is also composed by lenses of lacustrine and evaporite units that are also found in many small basins around Socompa. Therefore, it seems that the Salin Formation is characterized by medium to high permeability, being able to contribute a lot to the salinity of the infiltrating/circulating waters.

Since dacitic lava flow and domes younger than 7000 years BP are recognized, the Socompa volcano is classified as active volcano. Close to the summit, Socompa volcano exhibits cold and weak fumaroles and steaming ground with temperature close to 25°C. This temperature is close to the maximum temperature measured in thermal springs (25.7°C) and soil (23.5°C) in the west side of the Socompa lagoon. This characteristic suggests the presence of not negligible heat flow, which could be responsible, at least in part, for the heating of the waters through conductive transfer. This appears to be a rather widespread process, which testifies the considerable extension of the "thermal anomaly".

Chloride plots suggest that the water discharges around the Socompa lagoon are affected by freshwater-salty water mixing and/or interaction with salt deposits/incrustations. This process characterize also the springs discharging into the Llullaillaco salar. Thermal springs discharging in the Socompa lagoon and at the Quebrada del Agua have a maximum temperature respectively of 25.7°C and 18.0°C, whereas a TDS values are 15-20 meq/L and 2 meq/L. Generally speaking,

the thermalism is low, but can not be considered negligible taking into account the altitude and the mean annual temperature (-5°C; Houston J and Hartley A.J., 2003). Chemical and isotopic composition of sampled waters are not the same, suggesting different feeding zones and water flow paths.

Due to the chemical characteristics of thermal waters collected in this study (dilute and very immature waters) there are a little chance to obtain meaningful geothermometric estimations. The most suitable springs for the application of geothermometry seems to be those discharging in the Socompa lagoon. A combination of two chemical subsystems responding most rapidly to changes in temperatures (dissolved silica and the K^2/Mg ratio) suggest disequilibrium conditions between two subsystems. Based on the K^2/Mg ratio, temperature estimation is close to 60-70°C. Considering the saturation respect to chalcedony the estimation is close to 95°C even if collected waters show saturation conditions close to other silica polymorph (i.e. opal).

Stable isotopes compositions suggest a meteoric recharge for all collected waters, which are characterized by large variations in $\delta^{18}O$ and δD data. Although differences in stable isotopic composition of source water vapour and in infiltration altitude can explain part of the observed variations, others physical processes such as evaporation, sublimation and refreezing can be able to change deeply the pristine isotopic compositions. These processes seems to be active in the region, also outside the SGP, since waters located far from the Socompa lagoon (i.e. Llullaillaco salar and Punta Negra basin) show similar pattern and alignment in the classical δD vs $\delta^{18}O$ correlation plot. Taking into account these uncertainties, on the basis of available data the oxygen-18 shift cannot be considered as a responsible of the distribution of the points for collected thermal waters in the δD vs $\delta^{18}O$ correlation plot.

From the geochemical point of view, no geothermal end-member and/or reservoir were clearly identified in the SGP. Collected waters are classified as immature and geothermometric estimations could be affected by uncertainties. However, the lack of surface thermal manifestations and, more in general, of clear evidences of buried geothermal system is not necessary a negative indication, as blind geothermal systems were identified and exploited in the Andes (i.e. Cerro Pabellon). The SGP seems to be characterized by heat source and water availability.

This work provides new chemical and isotopic data regarding thermal and cold springs (some of these previously unknown) in the SGP and its neighborhood. The geochemical exploration performed has permitted to obtain new information regarding the hydrological/hydrogeological circuits and their mutual relationships. However, from this study a more complex system was highlighted and more data should be necessary in order to better

clarify the uncertainties arose, regarding the conceptual model of the study system (i.e. feeding zones, water flow path, water rock interaction processes, temperature estimation).

New sampling should concern the springs collected in April, but also searching for new ones (e.g. springs located at higher altitude around the Socompa lagoon). Others recommendations regard sampling of:

- the well identified in April in the plain between the Socompa lagoon and Quebrada del Agua;
- the Salin Formation (Sedimentita Vizcachera?) for isotopic characterization (^{13}C and ^{34}S). Other useful activity is represented by leaching tests addressed to the chemical characterization of the fluids obtained after the interaction with this salty deposits;
- fumaroles at the summit of the Socompa volcano (if safety conditions will be guaranteed);
- Llullaillaco salar in its central sector, after agreement with the mining company.

References

Alpers C. and Whittemore D. (1990). Hydrogeochemistry and stable isotopes of ground and surface waters from two adjacent closed basins, Atacama Desert, northern Chile. Applied Geochemistry, Vol.5, pp. 719-734.

Craig H. (1961). Isotopic variations in meteoric waters. Science, 133, pp. 1701-1703.

Cooper L.W., Solis C., Kane D.L. and Hinzman L.D.: Application of Oxygen-18 Tracer Techniques to Arctic Hydrol. Process, Arctic Alpine Res., 25, pp. 247-255., 1993.

Galliski M., Arias J.E., Coira B and Fuertes A. (1987). Reconocimiento geotermico del area Socompa, Provincia De Salta, Republica Argentina. Rev. Del Instituto de geologia y Mineria N°7 – UNJu. Republica Argentina.

Gat J.R. and Carmi I. (1970). Evolution of the isotopic composition of atmospheric waters in the Mediterranean Sea area. J. Geophys. Res., 75, pp. 3039-3048.

Giggenbach W.F. (1986). Graphical techniques for the evaluation of water/rock equilibration conditions by use of Na, K, Mg, Ca-contents of discharge waters. Proc. 8th New Zealand Geothermal Workshop, pp. 37-44.

Giggenbach W.F. (1988). Geothermal solute equilibria. Derivation of Na-K-Mg-Ca geoindicators. Geochimica et Cosmochimica Acta, vol. 52, pp. 2749-2765.

Giggenbach W.F. (1991b) Isotopic composition of geothermal water and steam discharges. In Application of Geochemistry in Geothermal Reservoir Development. (F. D'Amore, co-ordinator), UNITAR, 253-273.

Giggenbach WF (1992a) Isotopic shifts in waters from geothermal and volcanic systems along convergent plate boundaries and their origin. Earth Planet. Sci. Lett. 113, 495-510.

Giggenbach W.F., Sheppard D.S., Robinson B.W., Stewart M.K. and Lyon G.L. (1994). Geochemical structure and position of the Waiotapu geothermal field, New Zealand. Geothermics, vol. 23, pp. 599-644.

Houston J. and Hartley A.J. (2003). The central Andean West-slope rainshadow and its potential contribution to the origin of hyper-aridity in the Atacama Desert. Int. J. Climatol., 23, pp. 1453-1464.

Kendall C, and McDonnell J. (1998). Isotope tracers in catchment hydrology. Amsterdam: Elsevier.

Langelier W.F., and Ludwig H.F. (1942). Graphical methods for indicating the mineral character of natural waters. J.A. Water Works Assoc., 34: 335.

Ohlanders N., Rodriguez M., McPhee J. (2013). Stable isotope variation in a Central Andean watershed dominated by glacier and snowmelt. Hydrol. Earth Syst. Sci., 17, pp. 1035-1050.

Ramirez C.F. (1988). The geology of Socompa volcano and its debris avalanche deposit, northern Chile. MSc dissertation, Open University, Milton Keynes, UK.

Rodhe A. (1998). Snowmelt-dominated systems, in: Isotope tracers in catchment hydrology, edited by: Kendall, C. and McDonnell, J.J., Elsevier, Amsterdam, The Netherlands and Oxford, UK, 1998.

Taylor S., Feng. X., Kirchner J.W., Osterhuber R., Klaue B. and Renshaw C.E.: Isotopic evolution of a seasonal snowpack and its melt and became progressively enriched and the dependence can be reproduced the observed progressive, Water Resour. Res., 37, pp. 759-769, 2001.

Tonani F.B. (1982). Evaluation of geochemical data for Island of Nysiros. IGME report. Geochemical Project GRE/77/007, 19pp. (unpubl.).

Unnikrishna P.V., McDonnell J.J., and Kendall C.: Isotope variations in a Sierra Nevada snopack and their relation to meltwater, J. Hydrol., 260, pp. 38-57, 2002.

Wolery T.J. (1983). EQ3NR. A computer program for geochemical aqueous speciation-solubility calculations: user's guide and documentation. Lawrence Livermore Laboratory, Report UCRL-53414, 191 pp.

Wolery T.W. and Jarek R.L. (2003). Software user's manual. EQ3/6, Version 8.0, Sandia National Laboratories – U.S. Dept. of Energy.

Yurtsever Y. and Gat J.R. (1981). Atmospheric waters. In Stable Isotope Hydrology: Deuterium and Oxygen-18 in the Water Cycle (eds. J.R. Gat and R. Gonfiantini), IAEA Tech. Rep. Ser., 210, pp. 103-142.

Zappettini E. and Blasco G. (2001). Hoja Geológica 2569- II, Socompa, provincia de Salta. Instituto de Geología y Recursos Minerales, Servicio Geológico Minero Argentino, Boletín 260, Buenos Aires, 62 pp.

Annex 1

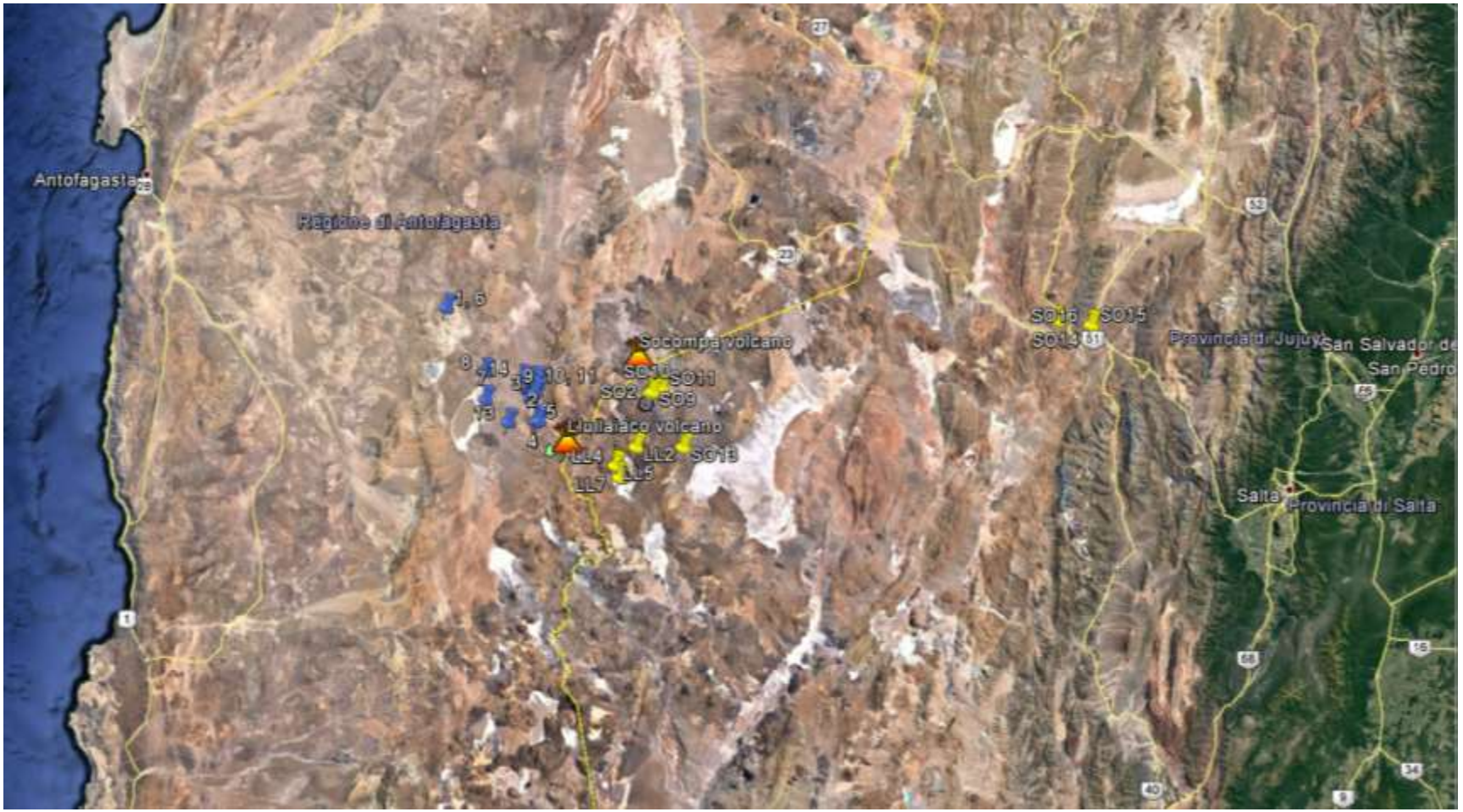

Fig.A1 – Location map of the studied area. Yellow symbols represent samples collected in this sampling trip (April, 2018), whereas blue symbols refer to data from Alpers and Whittemore, 1990.

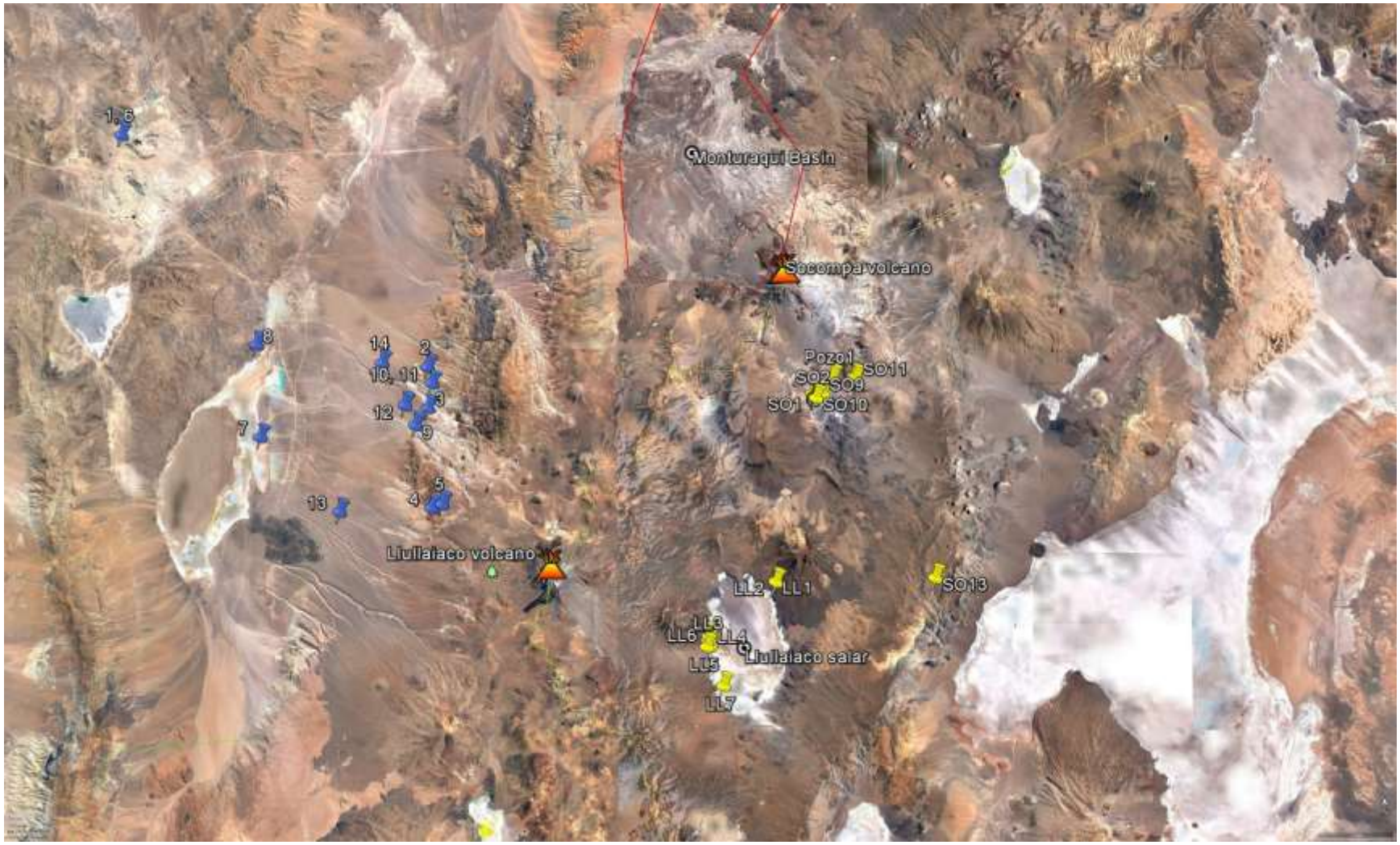

Fig.A2 – Location map of the water samples collected. Symbols as in figure 1.

Figure A3a. Sampling of cold spring dicharging in the Socompa lagoon

Figure A3b. Sampling of thermal spring dicharging in the Llullaillaco salar

Figure A4. Location map of sampling point around the Socompa lagoon.

Figure A5. Location map of sampling point around the Llullaillaco salar.

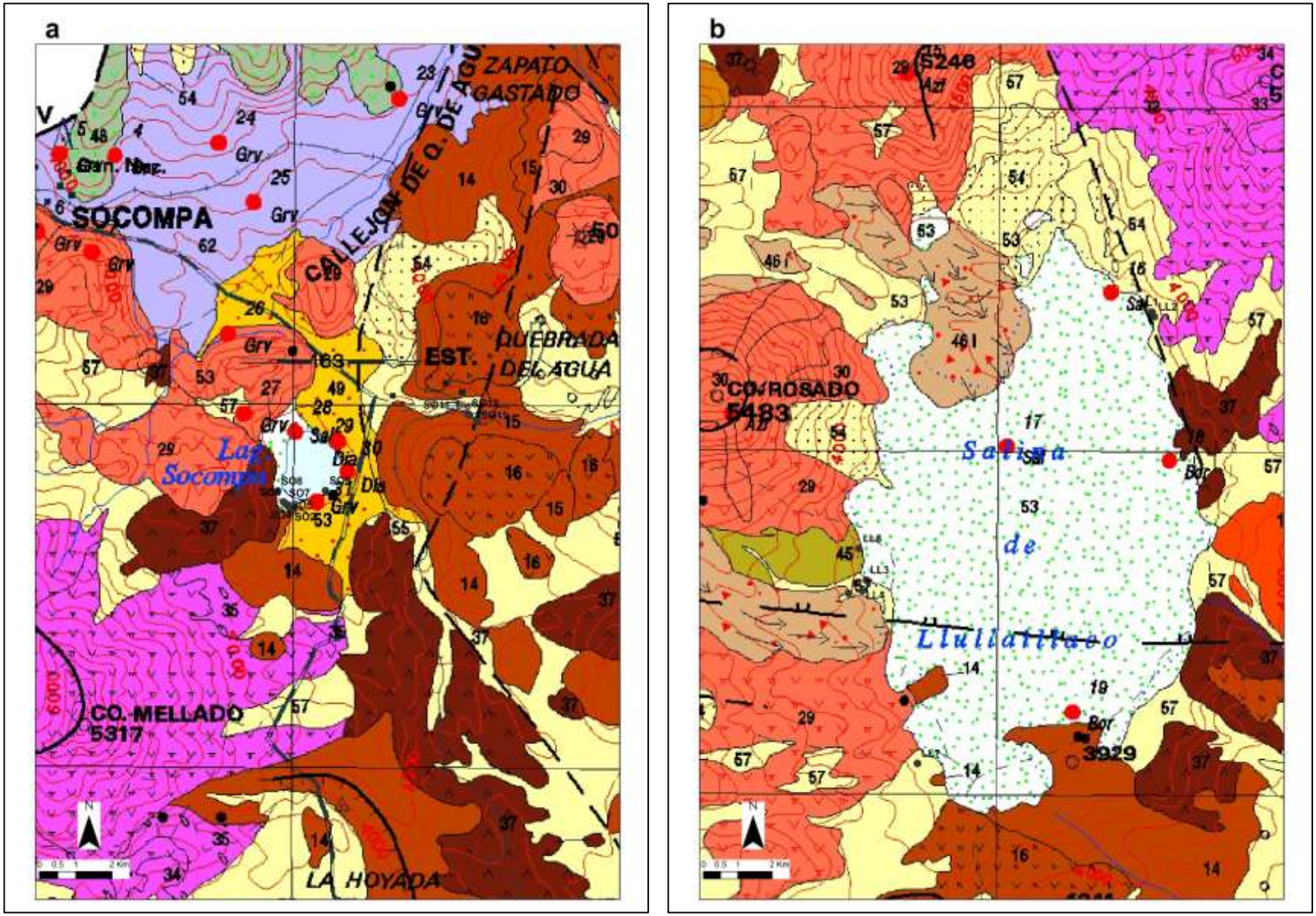

Figure A6. Geological map of the SGP (Zappettini and Blasco, 2001): a) Socompa lagoon, b) Llullaillaco salar

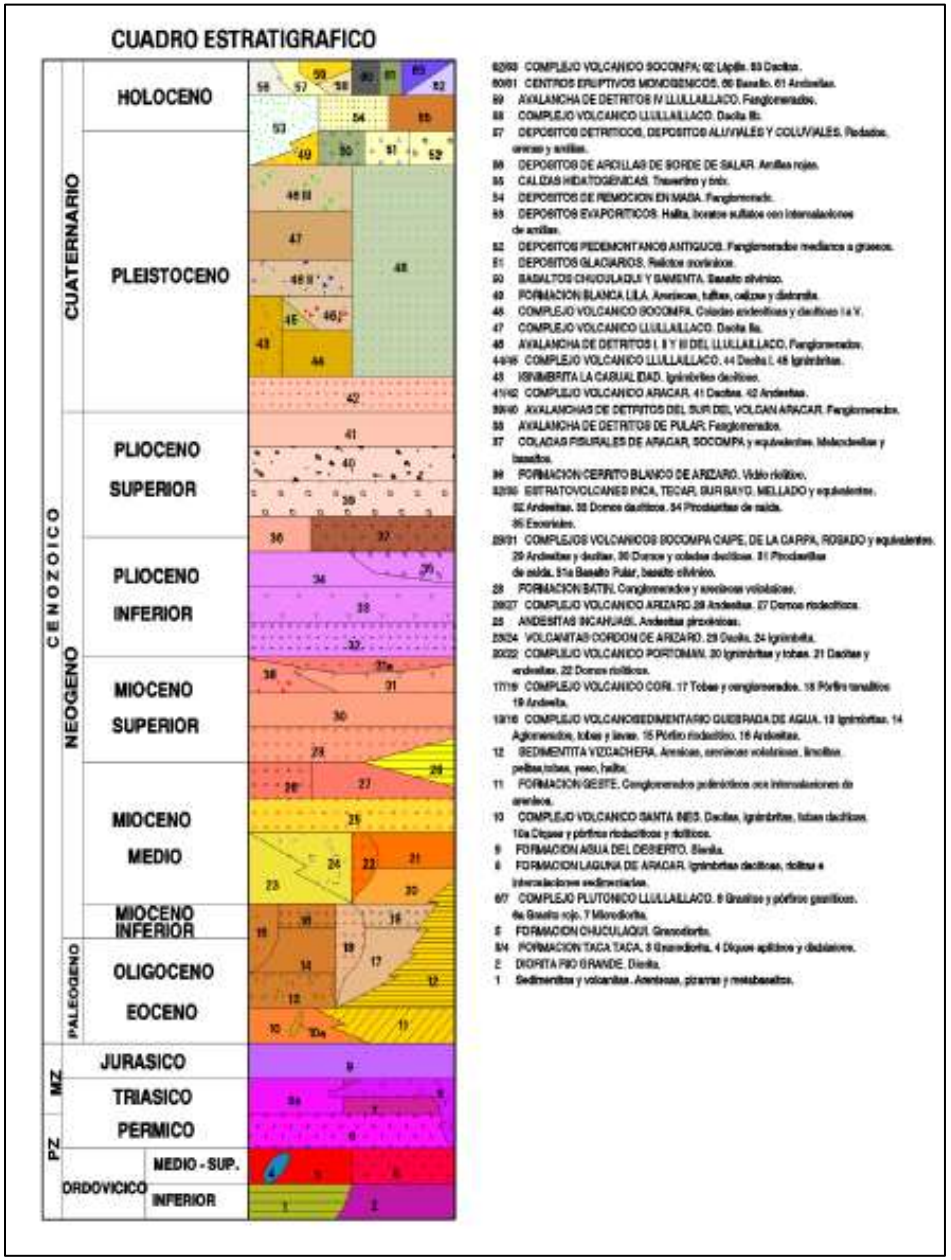

Figure A7. Legend of the geological map from Zappettini and Blanco (2001)